Surface Termination of Fe_3O_4(111) Films Studied by CO Adsorption Revisited

X. Li, J. Paier,* J. Sauer

Institut für Chemie, Humboldt-Universität zu Berlin, 10099 Berlin, Germany

F. Mirabella, E. Zaki, F. Ivars-Barceló, S. Shaikhutdinov,* H.-J. Freund

Fritz-Haber-Institut, Max Planck Society, Faradayweg 4-6, 14195 Berlin, Germany

ABSTRACT: Although the (111) surface of Fe_3O_4 (magnetite) has been investigated for more than twenty years, substantial controversy remains in the literature regarding the surface termination proposed based on structural and adsorption studies. The present paper provides density functional theory results that allow to rationalize experimental results of infrared reflection-absorption spectroscopy and temperature programmed desorption studies on CO adsorption, thus leading to a unified picture in which the Fe_3O_4(111) surface is terminated by a $^1/_4$ monolayer of tetrahedrally coordinated Fe^{3+} ions on top of a close-packed oxygen layer as previously determined by low energy electron diffraction. However, surface defects play a crucial role in adsorption properties and may dominate chemical reactions on Fe_3O_4(111) when exposed to the ambient.

1. INTRODUCTION

Due to their enormous importance in geology, physics, and chemistry, iron oxides in various compositions and structures and their surfaces, especially in contact with the environment, have been intensively studied.[1] Characterization of Fe_3O_4 (magnetite) surfaces, addressed in the present work, has come a long way. An excellent comprehensive review about the surface structures of iron oxides, following a much earlier one,[2] has recently been published.[3] This review considers the surface structure of the clean $Fe_3O_4(001)$ surface as solved. The situation is less clear for the $Fe_3O_4(111)$ surface. Low energy electron diffraction (LEED) studies, performed on $Fe_3O_4(111)$ thin films grown on Pt(111) and combined with scanning tunneling microscopy (STM) results, suggested a termination with a $^1/_4$ monolayer of (in the bulk) tetrahedrally coordinated Fe^{3+} ions over a close–packed oxygen layer (Fe_{tet1}; for nomenclature see Fig. 1).[4-5] This surface structure may be obtained by cutting along the Fe_{tet1} layer in the magnetite (inverse spinel) structure with surface Fe ions strongly relaxed inward. A recent LEED I/V study[6] reinforced this conclusion by providing a very reasonable reliability (Pendry R-) factor of ~0.1, and must be taken as strong evidence of a proper and hence solved surface structure. Also, the surface stability diagram based on density functional theory (DFT) calculations suggests the Fe_{tet1}-terminated surface to be most stable at experimentally relevant pressures and temperatures.[7-11] On the contrary, an adsorption study[12] using CO as a probe molecule as well as a very recent study on water interaction with $Fe_3O_4(111)$[13] were both rationalized in terms of a surface terminated by octahedrally coordinated iron ions (Fe_{oct2}; see Fig. 1) in the outermost layer.

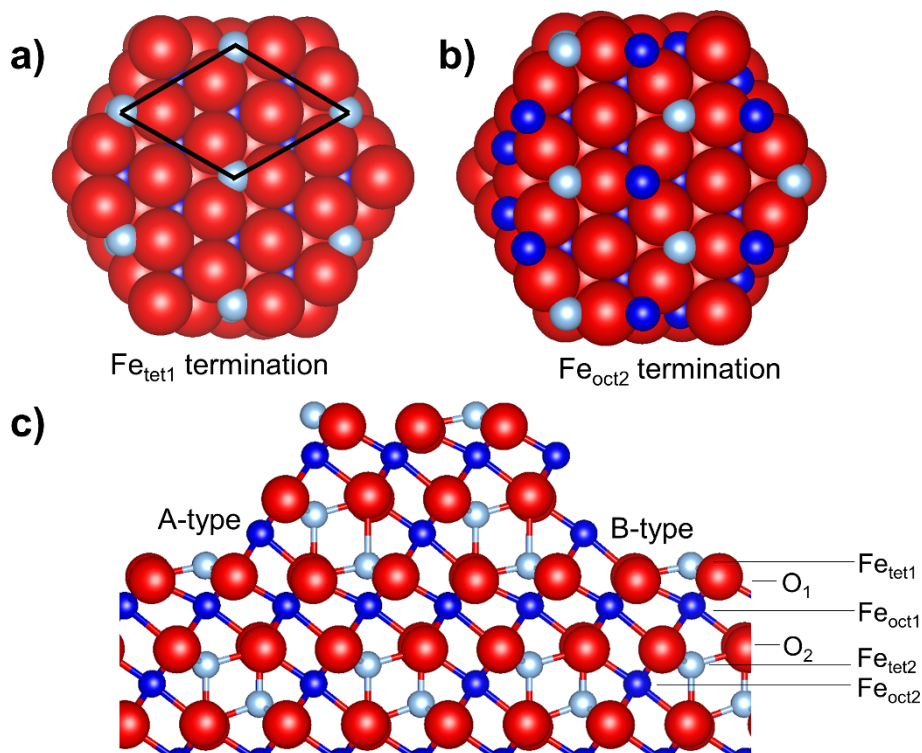**Figure 1.** Top views on the Fe_{tet1} (a) and Fe_{oct2} (b) terminated $Fe_3O_4(111)$ surface. Cross-view on a stepped $Fe_3O_4(111)$ surface (c) showing the two step types A and B. Regular stacking sequence along [111] of atomic layers are shown on the right-hand side. Tetrahedrally coordinated Fe^{3+} ions are light blue, octahedrally coordinated Fe^{2+} ions are dark blue, and oxygen is red.

Apparently, there is disagreement between surface structures derived from LEED and DFT studies on one hand and adsorption studies on the other. In the present work, we critically analyze the origin of this controversy and report DFT results, which allow us to provide a unified picture of the surface termination of $Fe_3O_4(111)$, in which the surface exposes a $^1/_4$ monolayer of tetrahedrally coordinated Fe^{3+} ions over a close-packed oxygen layer as previously determined by LEED.

2. METHODS AND MATERIALS

A. Experimental details. The experiments were carried out in several ultra-high vacuum (UHV) chambers with a background pressure below 5×10^{-10} mbar. All setups were equipped with standard facilities necessary to grow well-ordered thin magnetite films on clean Pt substrates. The quality of the films was checked by LEED which revealed sharp diffraction spots with low background intensity, and no other elements except Fe and O were observed in the Auger electron spectra (AES, both from Specs). The adsorption studies were performed via

temperature programmed desorption (TPD) using a differentially pumped quadrupole mass spectrometer (QMS, from Hiden) having a gold-plated cone shield to minimize signals from the heating stage. Vibrational spectra were measured by infrared reflection absorption spectroscopy (IRAS, Bruker 66 ivs). In one chamber, CO was dosed via calibrated molecular beam. In other setups, CO was dosed by back filling the chamber. CO exposures are given in Langmuirs (1 L = 10^{-6} Torr×sec). STM studies were performed in another UHV chamber equipped with LEED, AES and a scanning tunneling microscope (from Omicron) operated at room temperature.

The $Fe_3O_4(111)$ films, with a thickness of about 5 nm, were grown on Pt(111) following a well-documented recipe[4-6, 12] and will be discussed in detail in the text. Although the precise preparation parameters (Fe flux, oxidation temperature, time and oxygen pressure) used in each setup may slightly differ, all oxide films exhibited a high degree of order as judged by LEED. In addition, the samples prepared in different chambers showed similar TPD spectra of CO allowing for cross-correlation of the results obtained by different techniques.

Preparation of the $Fe_3O_4(001)$ films on Pt(001) is described elsewhere.[14] The films show sharp LEED patterns of the $Fe_3O_4(001)$-($\sqrt{2}\times\sqrt{2}$)R45° reconstructed surface and exhibit the same surface morphology as reported for a single crystal.[3]

TPD spectra were measured with a heating rate of 3 K/sec. IRA spectra were measured at grazing angle 8° with the resolution of 4 cm^{-1}. Note that the cooling time to reach the base temperature of 90 K is at least 5 minutes. STM images were recorded with commercial Pt-Ir tips (L.O.T. Oriel).

B. Computational details. The details of DFT calculations are amply discussed in ref. 11. In this section, we only report the most important points to be self-contained. DFT results were obtained using periodic slab models preserving the Fe_3O_4 composition. Primitive (1×1) surface unit cells were cut along the (111) crystallographic plane in the bulk. The equilibrium bulk lattice constant is determined by virtue of fitting a series of single points to the equation of state after Murnaghan.[15] It is 850.8 pm for the bulk and conveys to a surface unit cell vector length of 601.6 pm. Since this work compares two distinct surface terminations, we emphasize that respective slab models use identical compositions ($Fe_{12}O_{16}$), i.e 12 atomic layers with the single metal (Fe_{tet1}; see Fig. 1) termination as the topmost layer and the double metal (Fe_{oct2}; see Fig. 1) termination as the bottommost layer (and *vice versa*). We use so-called asymmetric models constraining the atomic coordinates of the four bottommost layers to the bulk values during

structure optimizations. Electronic structure calculations employ the so-called DFT+U[16] approach using a U value applied to the Fe 3d orbitals of 3.8 eV[9, 17] together with the Perdew, Burke, and Ernzerhof (PBE)[18] exchange-correlation functional. We use the VASP[19-20] code benefiting from the efficient projector-augmented wave method[21-22] to describe the electron-ion interaction on a full-potential level. The cutoff for the plane-wave basis set is 800 eV and Brillouin zones of surface unit cells are sampled for integration by a $(5 \times 5 \times 1)$ Γ-centered Monkhorst-Pack[23] k-point mesh. To calculate vibrational frequencies of adsorbed CO molecules, we employ normal mode analysis calculating the mass-weighted (partial) Hessian as the first derivative of atomic gradients with respect to their Cartesian components using central differences and a step size of 1.5 pm. Errors in wavenumbers incurred by the harmonic as well as the density functional approximation have been taken care of by scaling the wavenumber of $\nu(CO)$ in the free molecule (calc. 2123 cm^{-1}) with respect to the experimental value (2143 cm^{-1}).[24]

3. RESULTS AND DISCUSSION

A. Experimental results. Results of CO adsorption on $Fe_3O_4(111)$, obtained by TPD and IRAS, are shown in Fig. 2. CO was first dosed at 90 K to a certain coverage monitored by IRAS, and the TPD spectrum was then recorded upon heating to 600 K. This was repeated several times while stepwise increasing the coverage up to the saturation limit. Clearly CO molecules chemisorb in, at least, three distinct states, referred to as α, β and γ (see ref. 12). (Due to additional adsorption from residual gas during the time it takes to place the sample in front of the QMS, TPD spectra may correspond to a slightly higher CO coverage than measured in IRAS experiments). To further correlate the desorption peaks and the IRA bands, the IRA spectra were recorded at 90 K after thermal flash to the specified temperature (Fig. 2b). Both sets of experiments clearly show that the γ desorption state at ~ 240 K is associated with CO molecules showing a sharp band at 2204 cm^{-1}. Accordingly, the β state at ~ 180 K correlates with a broad band in the 2110 - 2095 cm^{-1} region, which remains after desorption of the weakest bonded CO in the α state. The band position at the highest coverage and hence corresponding to the α desorption state is very sensitive to the adsorption temperature and shifts from ~ 2090 cm^{-1} observed at 105 K to ~ 2070 cm^{-1} when adsorbed at 90 K. Note that this assignment of the α state differs from the previously reported one,[12] where it has been associated with a very weak band at 2141 cm^{-1}, i.e. very close to CO in the gas phase (2143 cm^{-1}). Note also that the intensity

of the β signal relative to γ is considerably smaller than previously reported.[12] In fact, the intensities of both β and γ signals vary from sample to sample (see also Figs. 2 and 6 in ref. 12), although all films showed sharp LEED patterns.
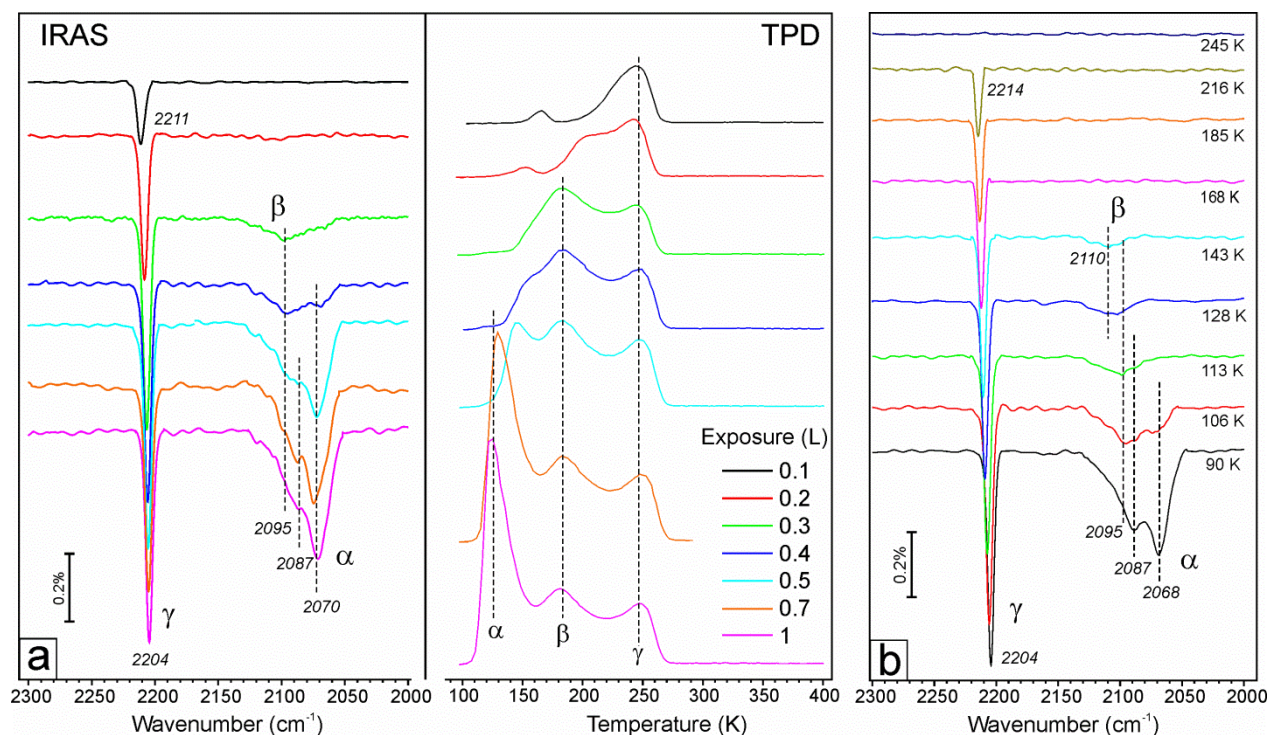

Figure 2. (a) Consecutive IRAS and TPD spectra (cut at 400 K) measured upon stepwise increasing CO dosage at 90 K on Fe_3O_4(111) films (see text). (b) IRAS spectra of 1 L CO at 90 K and after thermal flash to the temperatures as indicated. The film was prepared by oxidation at 1000 K and flashed to 800 K in UHV prior to CO adsorption. The spectra are offset for clarity.

To quantify the CO coverage in our films, we made use of CO TPD spectra obtained for the clean Pt(111) surface measured prior to film growth. The spectra (see Fig. 3) suggest about 0.25 monolayer (ML) for the CO coverage in total for the β and γ states. (1 ML is defined as 3.2×10^{14} atoms cm^{-2}, i.e. one atom per Fe_3O_4(111) unit cell). Obviously, this coverage cannot account for the regular surface and, therefore, must be assigned to defect sites. In addition, the β and γ states are often missing in the spectra for "as prepared" films and only appear if the sample is flashed to high temperatures prior to CO adsorption. Tentatively, this effect is attributed to adsorption of water, which is always present in the UHV background, that prevents CO adsorption in the γ state, as illustrated in Fig. S1 (ESI).
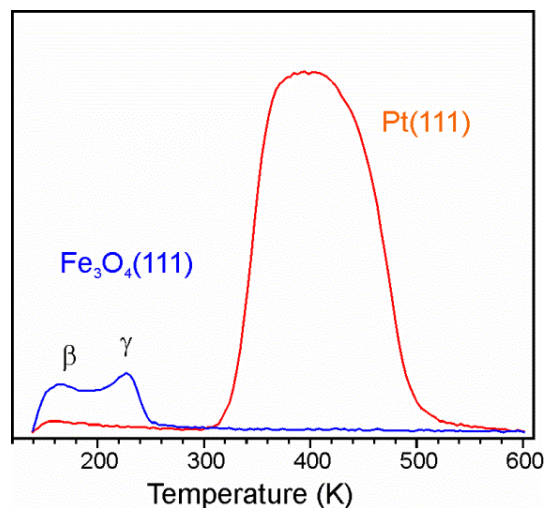
6

Figure 3. Comparison of TPD spectra of 1 L CO adsorbed on $Fe_3O_4(111)$ film and clean Pt(111) at 140 K measured with the same setup. CO adsorption on Pt(111) results in the c(4×2)-CO structure at CO density of 7.4×10^{14} cm^{-2}. Using this value for calibration, the integral area of β and γ signals corresponds to 8×10^{13} cm^{-2}, thus resulting in ~ 0.25 ML CO coverage (1 ML= 3.2×10^{14} cm^{-2}).

For comparison, Fig. 4 depicts a CO TPD spectrum obtained with the same setup on the clean (√2×√2)R45°-reconstructed surface of a $Fe_3O_4(001)$ film grown on Pt(001). This surface does not show any signature of strongly adsorbed CO. Apparently, the α state at around 100 K on both (111) and (001) surfaces is associated with the "tail" of CO desorption having a maximum at a considerably lower temperature, as was, indeed, observed in TPD experiments on a $Fe_3O_4(001)$ single crystal.

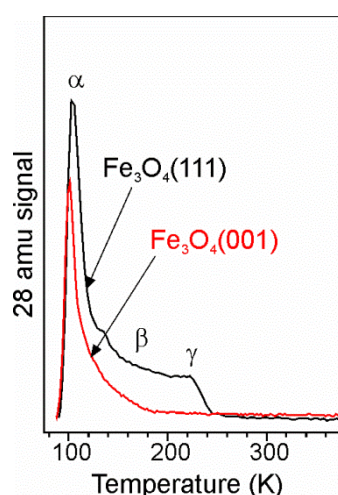**Figure 4.** TPD spectra of 1 L CO adsorbed on $Fe_3O_4(111)$ and $Fe_3O_4(001)$ films at 90 K. The (111) film was prepared by oxidation at 940 K.

Importantly, LEED and STM studies of the $Fe_3O_4(001)$-$(\sqrt{2}\times\sqrt{2})R45°$ surface both as thin films and single crystals revealed a uniform and atomically flat surface with a low amount of defects.[3, 14] Taking into account the relatively low intensities of the β and γ desorption states only present on the (111) surface, which, in turn, depend on film preparation (see also ref. 25) and vacuum conditions, it seems most likely that those are associated with surface imperfections, which are hard to control and quantify by conventional LEED usually employed to judge on the quality of the prepared films or single crystals.

Therefore, it is important to know the surface morphology of the prepared films (e.g. by STM) to link the CO adsorption results and the surface termination. Before we address STM results, it is instructive to look at the $Fe_3O_4(111)$ film preparation in more detail. The first step includes the formation of an FeO(111) monolayer film on the clean Pt(111) surface.[2] This step is easy to control by LEED and CO titration of Pt, which is also used for calibration of the Fe deposition flux. The next step involves several (3-5) cycles of Fe deposition in amounts equivalent to 5-10 monolayers of FeO(111) onto a substrate kept at room temperature or below (down to 100 K), followed by oxidation in 5×10^{-7} - 2×10^{-6} mbar of O_2 at 870-950 K for 5-10 minutes. In the final step, the films are oxidized at a slightly higher temperature, e.g. 930-1020 K for ca. 5 min. The final parameter to mention is the temperature, at which oxygen is pumped out, which is usually about 500 K, but may also be close to the oxidation temperature. Thus, there is a certain diversity in the film preparation which may, however, affect the adsorption results. In principle, this holds true for single crystal surfaces as well, see refs. 26 and 27.

STM studies show that all well-ordered films exhibit wide hexagonally- or trigonally-shaped terraces separated by monoatomic steps or step bunches (see Figs. 5a,b). STM images also revealed that oxidation at relatively high temperatures (~1000 K) and oxygen pumping out at 500 K, results in additional formation of small atomically flat islands (see Figs. 5b,c). Once formed, these islands could not be removed by re-oxidation at lower temperatures. Their formation is suppressed, however, if oxygen is pumped out simultaneously with sample cooling after high temperature oxidation at ~ 1000 K, or if the final oxidation is performed at relatively low temperatures (below 950 K). These islands, primarily of a trigonal shape, are all ~2.5 Å in height, that is about half of the distance between the equivalent layers in $Fe_3O_4(111)$ (= 4.6 Å), and must therefore expose a surface termination other than that of the surrounding terrace. The top facets showed no atomic corrugation, thus favoring its assignment to a surface which is terminated by the close-packed oxygen layer (i.e, O_2 layer; see Fig. 1c). Origin and driving force for the island formation are not well understood, and it seems hardly possible to judge on their presence or absence without STM inspection.
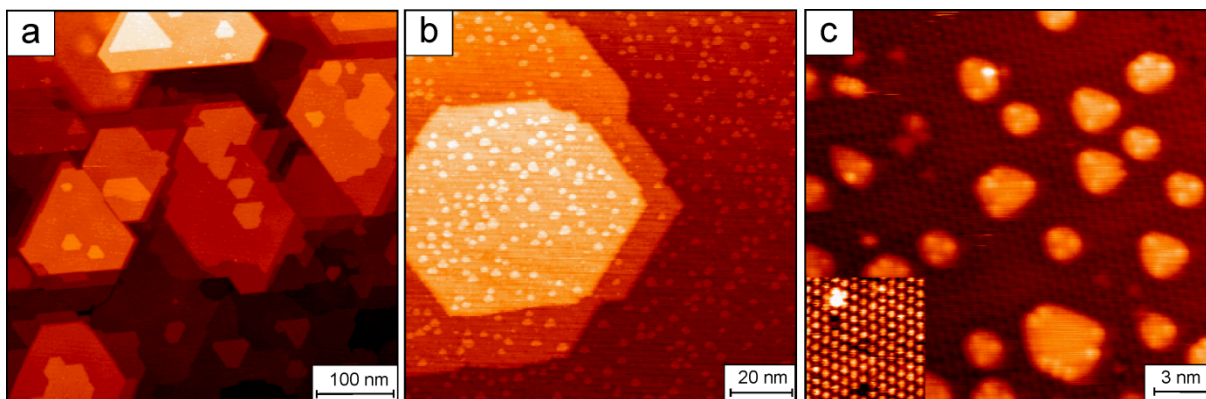
Figure 5. (a) STM image showing typical large-scale morphology of the $Fe_3O_4(111)$ films. When prepared by oxidation at ~1000 K, the films exhibit additional islands about 2.5 Å in height randomly distributed across the surface as shown in (b,c). The sample imaged in (c) was flashed to 800 K in UHV prior to imaging. The lattice of protrusions with a 6 Å periodicity is observed on the clean surface (see inset), which may additionally show adsorbate species (as bright protrusions) and vacancies (as missing protrusions). Tunneling conditions are: sample bias + 1.4 V, tunneling current 0.7 nA.

STM images of the adsorbate-free $Fe_3O_4(111)$ surface, which can only be obtained after thermal flash to 800 K (as for TPD/IRAS studies), showed a lattice of protrusions with 6 Å periodicity, i.e. one protrusion per unit cell, independent of bias polarity. Based on previous DFT calculations and image simulations,[5, 9] this picture corresponds to the single metal terminated surface, with the Fe_{tet1} ions being imaged as protrusions. For the double metal terminated surface, i.e. exposing the Fe_{oct2} - Fe_{tet1} layers, empty state STM images show one protrusion per unit cell, whereas filled state STM images show a honeycomb-like structure with two protrusions per unit cell, as observed on the $Fe_3O_4(111)$ single crystal surfaces after certain preparation treatments.[26, 28] Such images were never observed in our films at any tunneling conditions, thus suggesting that our films are Fe_{tet1}-terminated.

B. Computational results. According to DFT results published on thermodynamic stabilities of the various bulk terminations of $Fe_3O_4(111)$,[7-8] there is broad consensus (see ref. 8 and references therein) that under reducing conditions the Fe_{tet1} and Fe_{oct2} terminations (see Fig. 1c) are most stable, the first one distinctly more stable than the second one. The optimized structures **1** and **2** obtained for adsorption of CO on both surface terminations are displayed in Fig. 6. Structure **2** refers to CO adsorbed on the Fe_{oct2}^{2+} ion, which is by 76.5 kJ/mol more stable

9

than CO adsorbed on the Fe_{tet1}^{3+} ion of the Fe_{oct2} terminated surface. This is in qualitative agreement with results reported in ref. 29. Because one of the two iron ions binds CO so much stronger than the other, we only discuss structure **2** in the present work, i.e. CO adsorbed on the Fe_{oct2}^{2+} ion. Table 1 presents corresponding vibrational frequencies of the CO stretching mode together with adsorption energies obtained for 1 ML CO coverage, i.e. one CO molecule per (1×1) unit cell. Structures **3** and **4** represent crude models of step edges (defect sites) of type A and B, respectively, as shown in Fig. 1c.[12, 30] Model **3** features an oxygen layer on top of the Fe_{oct2} terminated surface and model **4** relates to the Fe_{oct1} terminated $Fe_3O_4(111)$ surface. Both models are built starting from the 12-atomic layer slab described in Sec. 2B. Note that additional O-layers in **3** and **4** are displayed in orange (see Fig. 6).

Table 1. Unscaled and scaled CO stretching frequencies (in cm⁻¹) and adsorption energies (in kJ/mol).

Structure	Termination	Ads. site[a]	ν(CO), cm⁻¹		E_{ads}	Experiment
			unscaled	scaled[b]	kJ/mol	
free CO	-	-	2123	2143	-	
1	Tet1	$Fe_{tet}^{3+}(4)$	2085	2105	−44.0	α
2	Oct2	$Fe_{oct}^{2+}(4)$	2030	2049	−102.6	-
3	Oct2	$Fe_{oct}^{2+}(6)$	2180	2200	−40.4	γ
4	Oct1	$Fe_{oct}^{2+}(5)$	2101	2121	−65.4	β

[a] Coordination number including CO is given in parenthesis.
[b] Scaling factor 1.0094 is obtained for free CO to fit the experimental value, i.e. 2143 cm⁻¹.[24]

The calculated and experimentally observed CO stretching frequencies are schematically shown for comparison in the top panel in Fig. 6. The comparison allows us to draw several conclusions:

1) First, the ν(CO) frequency obtained for the double metal termination (Fe_{oct2}^{2+}, 2049 cm⁻¹, structure **2**) is considerably lower than any of the observed frequencies. The pronounced red shift with respect to free CO may be explained by substantial d-π* back donation on the oxide surface.[31-32] In addition, adsorption on top of Fe_{oct}^{2+} results in a strongly exothermic adsorption energy of −102.6 kJ/mol, in qualitative agreement with previous results reported in ref. 29. In principle, such a strong CO binding would be consistent with the lower stability of the octahedrally terminated surface and the higher bond strength of CO to the Fe_{oct2} termination as predicted by DFT, if one considers a bond-order conservation picture.[7] However, the calculated adsorption energy (which is the highest among the structures considered) results in a CO desorption temperature of around 400 K (using classical Redhead analysis with a pre-factor of 10¹³ s⁻¹), which is, far outside the range of temperatures observed within the TPD spectra (see Figs. 2 and S1). Therefore, the comparison provides strong evidence that the surface is not octahedrally but tetrahedrally terminated.
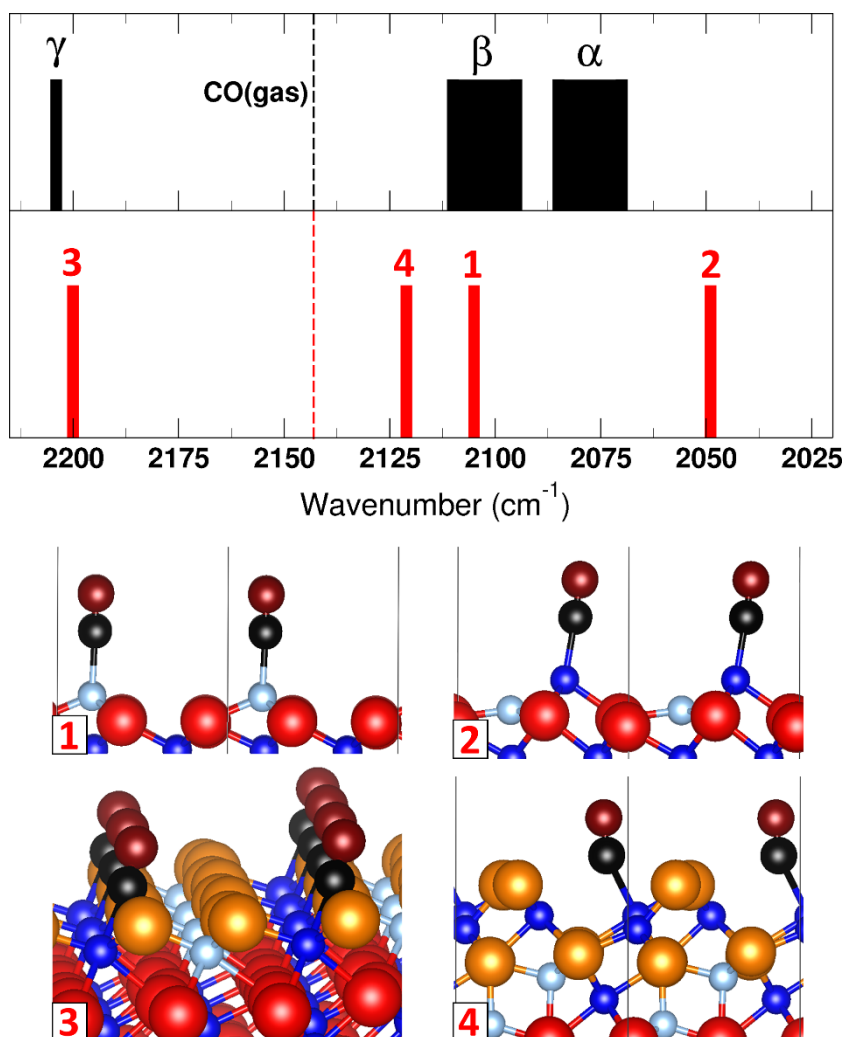
Figure 6. Comparison of experimentally observed and calculated ν(CO) bands for corresponding structures (**1-4**) shown below the spectrum. The Fe_{oct2} ions and Fe_{tet1} ions are shown in dark and light blue, respectively. Lattice oxygen is red; oxygen in O-adlayers (structures **3** and **4**) is orange; carbon is black; oxygen in CO is dark red.

2) The calculated frequency for structure **3** (2200 cm^{-1}) matches the γ peak (2204 cm^{-1}) well. The observed blue shift with respect to the gas phase CO is explained by the repulsive interaction between the electron lone pair of the C atom and the surface O^{2-} ions, also known as the "wall effect".[33] The geometric structure of step edges exposing such sites has previously been discussed using the criteria of charge neutrality and coordinative unsaturation.[30] DFT calculations, presented here, are consistent with this assignment. Moreover, the results clearly indicate that the blue-shifted ν(CO) bands cannot be explained in terms of CO adsorbed on the "naked" protruding Fe ions either in +2 or +3 oxidation states as shown in Table 1. Instead, such bands are anticipated for Fe ions "embedded" into the O layer providing the appropriate environment for Pauli repulsion.

12

3) The spectral region between 2110 and 2070 cm^{-1} exhibits more complex features. In principle, the frequencies calculated for the Fe$_{tet1}$-terminated surface (2105 cm^{-1}, model **1**) and Fe-exposing step edge (2120 cm^{-1}, model **4**) both fall into the experimentally observed region. However, based on relative peak positions, we assign the β state to CO adsorption on "Fe-rich" step edges (B-type, see Fig. 1c). It is the α state that dominates the spectra at low temperatures (see Fig. 2), which corresponds to the regular, Fe$_{tet1}$- terminated surface. The related band position is very sensitive to the adsorption temperature and may shift from 2090 cm^{-1} observed at 100 K to 2070 cm$^{-1,}$ when adsorbed at 90 K. This is an indication of a coverage effect. In addition, the α state is only populated at temperatures below the Verwey transition (~125 K), where charge ordering[34] may affect the vibrational frequencies.

4. CONCLUSIONS

CO as a probe molecule on oxide surfaces is a useful tool to elucidate the complex surface morphology, but assignment to specific adsorption sites is impossible without theoretical calculations. The CO stretching vibrations are sensitive to the adsorption site's local atomic as well as electronic structures. Our DFT results combined with experimental data provide firm evidence that the regular Fe$_3$O$_4$(111) surface is terminated by a ¼ monolayer of Fe$_{tet1}$ ions over close packed oxygen layer, in full agreement with previous LEED I/V results and thermodynamic stability of this surface predicted by DFT.

It therefore appears that the previously reported scheme for water adsorption[13] must be revisited. Although the proposed mechanism leading to a half-dissociated water dimer can still be operative, the existence of a clean double metal terminated surface in our films seems unlikely. Therefore, the water adsorption on the regular Fe$_3$O$_4$(111) surface must be rationalized in terms of the surface terminated by Fe$_{tet1}$, albeit the role of defects such as step edges must be considered for the initial stages of water interaction. Surface defects may play a crucial role in adsorption properties and may dominate chemical reactions on Fe$_3$O$_4$(111) when exposed to the ambient.

Finally, it is worth mentioning that a recent study on thin films of Co$_3$O$_4$(111) reached the conclusion that the surface is terminated by a ¼ monolayer of tetrahedrally coordinated Co^{2+} ions.[35] It therefore appears that both Fe$_3$O$_4$ and Co$_3$O$_4$ sharing the spinel structure show a preference to grow in (111) orientation with a surface terminated by a single metal cation. However, all observed CO bands[36] (i.e. 2155 - 2175 cm^{-1}) are blue-shifted with respect to the

gas phase, which in the case of magnetite would be only possible for the "O-rich" surfaces. In this case CO may adsorb on the metal cation and would repulsively interact with the surrounding oxygen (leading to a blue shift), as demonstrated for structure **3** (see Fig. 6). Corresponding DFT calculations, which are expected to be even more demanding than for iron oxide, would probably shed light on this issue. We point out that the DFT results of the present work do not examine all possible defect structures, but serve, in our opinion, as a good benchmark for further studies.

ASSOCIATED CONTENT

Supporting Information

The Supporting Information is available free of charge on the ACS Publication website at DOI: xxx.xxx

> Effects of residual water on CO adsorption.

AUTHOR INFORMATION

Corresponding Authors

*Phone +(49)-30-8413-4114. E-mail shamil.shaikhutdinov@fhi-berlin.mpg.de

*Phone +(49)-30-2093-7139. E-mail joachim.paier@chemie.hu-berlin.de.

Notes

The authors declare no competing financial interest.

REFERENCES

(1)   Cornell, R. M.; Schwertmann, U., *The iron oxides*; Wiley-VCH Verlag GmbH & Co. KGaA, 2004.

(2)   Weiss, W.; Ranke, W., Surface chemistry and catalysis on well-defined epitaxial iron-oxide layers. *Prog. Surf. Sci.* **2002**, *70*, 1-151.

(3)   Parkinson, G. S., Iron oxide surfaces. *Surf. Sci. Rep.* **2016**, *71*, 272-365.

(4)   Ritter, M.; Weiss, W., Fe_3O_4(111) surface structure determined by LEED crystallography. *Surf. Sci.* **1999**, *432*, 81-94.

(5)   Shaikhutdinov, S. K.; Ritter, M.; Wang, X. G.; Over, H.; Weiss, W., Defect structures on epitaxial Fe_3O_4(111) films. *Phys. Rev. B* **1999**, *60*, 11062-11069.

(6)   Sala, A.; Marchetto, H.; Qin, Z. H.; Shaikhutdinov, S.; Schmidt, T.; Freund, H. J., Defects and inhomogeneities in Fe_3O_4(111) thin film growth on Pt(111). *Phys. Rev. B* **2012**, *86*, 155430.

(7)   Kiejna, A.; Ossowski, T.; Pabisiak, T., Surface properties of the clean and Au/Pd covered Fe_3O_4(111): DFT and DFT+U study. *Phys. Rev. B* **2012**, *85*, 125414.

(8)   Noh, J.; Osman, O. I.; Aziz, S. G.; Winget, P.; Brédas, J.-L., Magnetite Fe_3O_4 (111) surfaces: Impact of defects on structure, stability, and electronic properties. *Chem. Mater.* **2015**, *27*, 5856-5867.

(9)   Yu, X.; Huo, C.-F.; Li, Y.-W.; Wang, J.; Jiao, H., Fe_3O_4 surface electronic structures and stability from GGA+U. *Surf. Sci.* **2012**, *606*, 872-879.

(10)   Santos-Carballal, D.; Roldan, A.; Grau-Crespo, R.; de Leeuw, N. H., A DFT study of the structures, stabilities and redox behaviour of the major surfaces of magnetite Fe_3O_4. *Phys. Chem. Chem. Phys.* **2014**, *16*, 21082-21097.

(11)   Li, X.; Paier, J., Adsorption of Water on the Fe_3O_4(111) Surface: Structures, Stabilities, and Vibrational Properties Studied by Density Functional Theory. *J. Phys. Chem. C* **2016**, *120*, 1056-1065.

(12)   Lemire, C.; Meyer, R.; Henrich, V. E.; Shaikhutdinov, S.; Freund, H. J., The surface structure of Fe_3O_4(111) films as studied by CO adsorption. *Surf. Sci.* **2004**, *572*, 103-114.

(13)   Dementyev, P.; Dostert, K.-H.; Ivars-Barceló, F.; O'Brien, C. P.; Mirabella, F.; Schauermann, S.; Li, X.; Paier, J.; Sauer, J.; Freund, H.-J., Water interaction with iron oxides. *Angew. Chem. Int. Ed.* **2015**, *127*, 14148-14152.

(14)   Davis, E. M.; Zhang, K.; Cui, Y.; Kuhlenbeck, H.; Shaikhutdinov, S.; Freund, H. J., Growth of Fe_3O_4(001) thin films on Pt(100): Tuning surface termination with an Fe buffer layer. *Surf. Sci.* **2015**, *636*, 42-46.

(15)   Murnaghan, F. D., The compressibility of media under extreme pressures. *Proc. Natl. Acad. Sci. USA* **1944**, *30*, 244-247.

(16)   Dudarev, S. L.; Botton, G. A.; Savrasov, S. Y.; Humphreys, C. J.; Sutton, A. P., Electron-energy-loss spectra and the structural stability of nickel oxide: An LSDA+U study. *Phys. Rev. B* **1998**, *57*, 1505-1509.

(17)   Yu, X.; Li, Y.; Li, Y.-W.; Wang, J.; Jiao, H., DFT+U study of molecular and dissociative water adsorptions on the Fe_3O_4(110) surface. *J. Phys. Chem. C* **2013**, *117*, 7648-7655.

(18)   Perdew, J. P.; Burke, K.; Ernzerhof, M., Generalized gradient approximation made simple. *Phys. Rev. Lett.* **1996**, *77*, 3865-3868; Erratum: **1997**, *78*, 1396-1396.

(19)   Kresse, G.; Furthmüller, J., Efficient iterative schemes for ab initio total-energy calculations using a plane-wave basis set. *Phys. Rev. B* **1996**, *54*, 11169-11186.

(20)   Kresse, G.; Furthmüller, J., Efficiency of ab-initio total energy calculations for metals and semiconductors using a plane-wave basis set. *Comp. Mater. Sci.* **1996**, *6*, 15-50.

(21)   Blöchl, P. E., Projector augmented-wave method. *Phys. Rev. B* **1994**, *50*, 17953-17979.

(22)   Kresse, G.; Joubert, D., From ultrasoft pseudopotentials to the projector augmented-wave method. *Phys. Rev. B* **1999**, *59*, 1758-1775.

(23)   Monkhorst, H. J.; Pack, J. D., Special points for Brillouin-zone integrations. *Phys. Rev. B* **1976**, *13*, 5188-5192.

(24)   Mantz, A. W.; Watson, J. K. G.; Rao, K. N.; Albritton, D. L.; Schmeltekorf, A. L.; Zare, R. N., Rydberg-Klein-Rees potential for $X^1 \Sigma^+$ state of CO molecule. *J. Mol. Spectrosc.* **1971**, *39*, 180.

(25)   Savara, A., Vibrational spectra of CO adsorbed on oxide thin films: A tool to probe the surface defects and phase changes of oxide thin films. *J. Vac. Sci. Technol. A* **2014**, *32*, 021505.

(26)   Lennie, A. R.; Condon, N. G.; Leibsle, F. M.; Murray, P. W.; Thornton, G.; Vaughan, D. J., Structures of $Fe_3O_4(111)$ surfaces observed by scanning tunneling microscopy. *Phys. Rev. B* **1996**, *53*, 10244-10253.

(27)   Cutting, R. S.; Muryn, C. A.; Vaughan, D. J.; Thornton, G., Substrate-termination and H_2O-coverage dependent dissociation of H_2O on $Fe_3O_4(111)$. *Surf. Sci.* **2008**, *602*, 1155-1165.

(28)   Shimizu, T. K.; Jung, J.; Kato, H. S.; Kim, Y.; Kawai, M., Termination and Verwey transition of the (111) surface of magnetite studied by scanning tunneling microscopy and first-principles calculations. *Phys. Rev. B* **2010**, *81*, 235429.

(29)   Huang, D.-M.; Cao, D.-B.; Li, Y.-W.; Jiao, H., Density function theory study of CO adsorption on $Fe_3O_4(111)$ surface. *J. Phys. Chem. B* **2006**, *110*, 13920-13925.

(30)   Henrich, V. E.; Shaikhutdinov, S. K., Atomic geometry of steps on metal-oxide single crystals. *Surf. Sci.* **2005**, *574*, 306-316.

(31)   Chatt, J.; Duncanson, L. A., Olefin co-ordination compounds .3. Infra-red spectra and structure - attempted preparation of acetylene complexes. *J. Chem. Soc.* **1953**, 2939-2947.

(32)   Blyholder, G., Molecular orbital view of chemisorbed carbon monoxide. *J. Phys. Chem.* **1964**, *68*, 2772.

(33)   Pacchioni, G.; Cogliandro, G.; Bagus, P. S., Characterization of oxide surfaces by infrared-spectroscopy of adsorbed carbon-monoxide - a theoretical investigation of the frequency-shift of CO on MgO and NiO. *Surf. Sci.* **1991**, *255*, 344-354.

(34)   Jeng, H. T.; Guo, G. Y.; Huang, D. J., Charge-orbital ordering and Verwey transition in magnetite. *Phys. Rev. Lett.* **2004**, *93*, 156403.

(35)   Heinz, K.; Hammer, L., Epitaxial cobalt oxide films on Ir(100)-the importance of crystallographic analyses. *J. Phys.: Condens. Matter* **2013**, *25*, 173001.

(36)   Ferstl, P., et al., Adsorption and activation of CO on $Co_3O_4(111)$ thin films. *J. Phys. Chem. C* **2015**, *119*, 16688-16699.